Available online at www.sciencedirect.com
SCIENCE DIRECT
Surface Science 600 (2006) 1497–1503
SURFACE SCIENCE
www.elsevier.com/locate/susc

Low temperature adsorption of oxygen on reduced $V_2O_3(0001)$ surfaces

M. Abu Haija [a], S. Guimond [a], Y. Romanyshyn [a], A. Uhl [a], H. Kuhlenbeck [a,*], T.K. Todorova [b], M.V. Ganduglia-Pirovano [b], J. Döbler [b], J. Sauer [b], H.-J. Freund [a]

[a] *Fritz-Haber-Institut der Max-Planck-Gesellschaft, Abteilung Chemische Physik, Faradayweg 4-6, 14195 Berlin, Germany*
[b] *Humboldt-Universität, Institut für Chemie, Unter den Linden 6, 10099 Berlin, Germany*

Received 8 December 2005; accepted for publication 3 February 2006
Available online 23 February 2006

Dedicated to Professor Volker Staemmler on the occasion of his 65th birthday

Abstract

Well ordered $V_2O_3(0001)$ films were prepared on Au(111) and W(110) substrates. These films are terminated by a layer of vanadyl groups under typical UHV conditions. Reduction by electron bombardment may remove the oxygen atoms of the vanadyl layer, leading to a surface terminated by vanadium atoms. The interaction of oxygen with the reduced $V_2O_3(0001)$ surface has been studied in the temperature range from 80 to 610 K. Thermal desorption spectroscopy (TDS), infrared reflection absorption spectroscopy (IRAS), high resolution electron energy loss spectroscopy (HREELS), X-ray photoelectron spectroscopy (XPS), and density functional theory (DFT) were used to study the adsorbed oxygen species. Low temperature adsorption of oxygen on reduced $V_2O_3(0001)$ occurs both dissociatively and molecularly. At 90 K a negatively charged molecular oxygen species is observed. Upon annealing the adsorbed oxygen species dissociates, re-oxidizing the reduced surface by the formation of vanadyl species. Density functional theory was employed to calculate the structure and the vibrational frequencies of the O_2 species on the surface. Using both cluster and periodic models, the surface species could be identified as η^2-peroxo (O_2^{2-}) lying flat on surface, bonded to the surface vanadium atoms. Although the O–O vibrational normal mode involves motions almost parallel to the surface, it can be detected by infrared spectroscopy because it is connected with a change of the dipole moment perpendicular to the surface.

Keywords: Thermal desorption spectroscopy; X-ray photoelectron spectroscopy; Infrared absorption spectroscopy; High resolution electron energy loss spectroscopy; Density functional theory; $V_2O_3(0001)$/Au(111); $V_2O_3(0001)$/W(110); Oxygen; Thin films; Phonons; Electronic structure; Adsorption

1. Introduction

Vanadium oxides are widely used in technological applications, such as electrical and optical switching devices, light detectors, critical temperature sensors and write–erase materials [1,2]. In addition to that, vanadium oxides are extremely interesting from a chemical point of view since they are active catalysts for a number of reactions like selective oxidation, selective reduction, and dehydrogenation of hydrocarbons and other organic compounds [1,2].

The interaction of oxygen with oxide catalysts is an important step in oxidation reactions of alkanes [3,4]. In an earlier publication Iwamoto and Lunsford pointed out that hydrocarbon oxidation reactions depend noticeably on the nature of the surface oxygen species formed during the interaction of oxygen with the oxide surface [5]. Therefore, an understanding of the nature of chemisorbed oxygen species is an important prerequisite for an understanding of catalytic reactions involving oxygen.

O_2^-, O_2^{2-}, O^- and O^{2-} species have been identified on oxide surfaces [5–15], their reactivity has been studied and

* Corresponding author. Tel.: +49 (0)30 8413 4222.
E-mail address: kuhlenbeck@fhi-berlin.mpg.de (H. Kuhlenbeck).

0039-6028/$ - see front matter © 2006 Elsevier B.V. All rights reserved.
doi:10.1016/j.susc.2006.02.003

their properties have been documented [16,17]. Their formation is caused by stabilization of oxygen molecules on coordinatively unsaturated (cus) cation sites where the degree of coordination and typically also the oxidation state is lower than that of regular sites. In an ionic picture, the oxygen adsorption process is accompanied by an electron transfer from the cus site with excess electron density into the oxygen molecule. Charged molecular forms of oxygen are unstable at high temperatures, tending to decompose upon heating and to re-oxidize the reduced oxide [7]. O_2^- (superoxo) species have been identified on oxide systems such as MgO [5], La_2O_3 [8], Bi_2O_3 [12], SnO_2 [13] and CeO_2 [14]. O_2^{2-} (peroxo) was identified on CeO_2 [18], SnO_2 [13], $SrTiO_3(100)$ [19] and Li doped NiO thin films [20,21]. Additional systems may be found in Refs. [6,7] and [17].

In the present work, oxygen chemisorption on the reduced $V_2O_3(0\,0\,0\,1)$ surface has been studied using TDS, XPS, IRAS and HREELS. Density functional theory was employed to model the vibrational properties of the adsorbed oxygen species and to identify the adsorbed species via comparison with the experimental data.

2. Experimental

X-ray photoelectron spectroscopy was performed at the BESSY II synchrotron radiation center in Berlin. The photoelectron spectra were recorded in an ultra-high vacuum (UHV) chamber equipped with a Scienta SES200 analyzer, which was mounted at an angle of 55° with respect to the incident photon beam. The overall energy resolution was usually better than 100 meV. XPS spectra of the V2p and O1s levels were taken with a photon energy of 630 eV. At this photon energy, the kinetic energy of the electrons is around 100 eV leading to high surface sensitivity. The energy scale was calibrated relative to the energy of the $W4f_{7/2}$ level by taking spectra of the tungsten filament used for sample heating. 120 eV photons were employed to excite valence band electrons.

Vibrational spectra were recorded in another chamber equipped with facilities for low-energy electron diffraction (LEED), TDS, IRAS and HREELS. High resolution electron energy loss spectra were recorded with a Delta 0.5 HREELS spectrometer (VSI GmbH). All spectra presented here were recorded in specular geometry with an incidence angle of 65° relative to the surface normal. The primary electron energy was set to 5 eV and the energy resolution was about 30 cm^{-1}. Infrared absorption spectra were obtained with a modified Mattson RS-1 FTIR spectrometer. The angle of incidence of the IR light relative to the sample normal was about 85°. IR spectra were usually obtained by accumulating 500 scans with a resolution of 2 cm^{-1}.

The samples were mounted using tantalum and tungsten wires attached to a hollow rod which could be filled with liquid nitrogen for cooling purposes. Temperatures of 88 K could be reached. In the case of the IRAS/HREELS/TDS system the sample was heated by passing an electrical current through the wires holding the sample whereas in the other system a tungsten filament mounted behind the backside of the sample was used for heating via electron irradiation or thermal radiation for not too high temperatures. Electron beam heating was only employed for sample preparation but not in the course of the *oxygen adsorption* experiments to prevent unintentional surface reduction. A tungsten–rhenium (26%/5%) thermocouple spot-welded to the sample was used for temperature control in the case of the W(1 1 0) substrate. The temperature of the Au(1 1 1) crystal was measured with a chromel/alumel thermocouple inserted into a small hole drilled into the crystal's side.

Au(1 1 1) was cleaned in UHV by cycles of argon sputtering and annealing at 1050 K. To remove carbon from W(1 1 0) the usual cleaning cycles were performed. One cycle consists of heating the sample to 1800 K in 1×10^{-6} mbar of oxygen for a few minutes followed by annealing at 2300 K in vacuum.

The $V_2O_3(0\,0\,0\,1)$ film on Au(1 1 1) was prepared by evaporation of metallic vanadium (using an Omicron EFM3 electron beam evaporator) in an oxygen atmosphere (1×10^{-7} mbar) at 600 K followed by annealing at 670 K in 1×10^{-7} mbar of oxygen and annealing in vacuum at 850 K. In the case of the W(1 1 0) substrate vanadium was evaporated (using an Omicron EFM4 electron beam evaporator) at 650 K in an oxygen atmosphere of 2×10^{-7} mbar followed by annealing at 800 K in 2×10^{-7} mbar of oxygen. In both cases very similar LEED patterns of the oxide layers were observed. The evaporators were calibrated using a quartz microbalance. Evaporation rates between 0.5 and 1 Å/min were employed in the experiments. The prepared $V_2O_3(0\,0\,0\,1)$ films were usually about 100 Å thick.

3. DFT calculations

For the calculations on the periodic slab model a plane-wave basis set with an energy cutoff of 400 eV, a $(6 \times 6 \times 1)$ *k*-point grid, and the PW91 exchange-correlation functional [22] as implemented in the Vienna ab initio Simulation Package (VASP) [23,24] were used. The interaction between the ionic cores and the valence electrons was described by the projector augmented wave (PAW) method [25,26]. All atoms were allowed to relax. Harmonic vibrational frequencies were calculated by numerical differentiation of forces using 0.02 Å displacements in both directions.

For the finite cluster models all-electron calculations were made using the TURBOMOLE 5.6 code [27,28] with the triple-zeta valence plus polarization (TZVP) basis set of Ahlrichs and co-workers [29] and the PBE functional [30]. Harmonic vibrational frequencies were calculated from analytical second derivatives of the energy [31].

4. Results and discussion

It has been shown previously by HREELS, IRAS and XPS that reduction of the vanadyl terminated

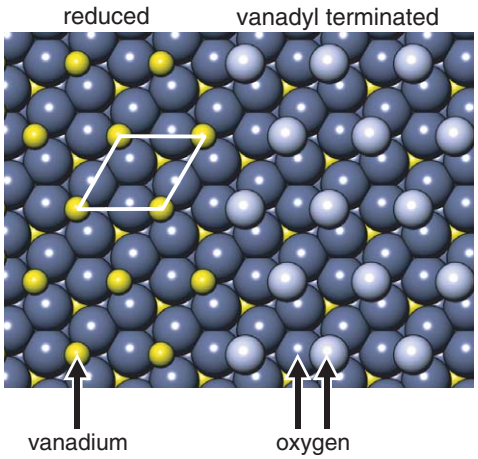

Fig. 1. Structure of the reduced and the vanadyl terminated surface. The surface unit cell is indicated.

$V_2O_3(0001)$ surface by electron irradiation leads to removal of the vanadyl oxygen atoms [32]. The structures of the vanadyl terminated and the reduced surface are displayed in Fig. 1. STM images of the vanadyl terminated surface have been published by Schoiswohl et al. [33]. For the reduced surface it has been assumed that the surface is terminated by vanadium atoms [32]. Preliminary results of STM studies show that the surface is largely ordered and flat with 10–20% of the surface area covered by defects [34,35].

XPS data for the interaction of oxygen with reduced $V_2O_3(0001)$ are shown in Fig. 2. Oxygen exposure at 80 K immediately leads to a significant decrease of the V3d intensity [Fig. 2(B), spectrum (β)]. In an ionic picture the V3d electrons would be the vanadium valence electrons not involved in the V–O bonding. This picture is surely not fully suited to describe the bonding within vanadium oxides since there are significant covalent contributions but calculations [1] show that the occupation of the V3d level varies with the vanadium oxidation state similar to what the ionic picture would predict. UPS experiments performed for different vanadium oxides [35] indicate that this relationship also holds for the V3d intensity which is related to the V3d occupation via photoemission cross sections. Therefore changes of the V3d intensity may be used as an indication for changes of the effective oxidation state (we call it *effective* oxidation state since the oxidation state corresponding to the V3d occupation would possibly not be represented by an integer number). In this context the decrease of the V3d intensity in Fig. 2(B) (β) indicates that the *effective* oxidation state of the surface vanadium atoms increases upon O_2 dosage at 80 K. Spectra (γ) to (ε) also point towards an increased vanadium oxidation state. The same conclusion may be drawn from the shift

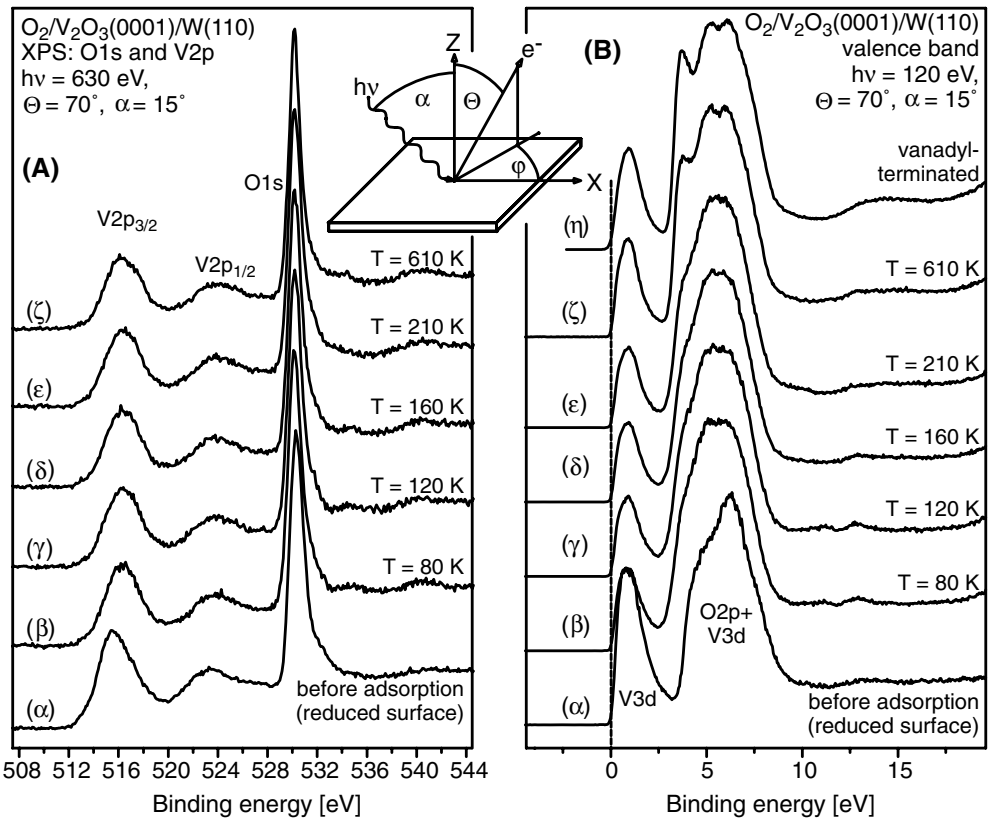

Fig. 2. Photoelectron spectra obtained after annealing a reduced $V_2O_3(0001)/W(110)$ surface at different temperatures after exposure to O_2. The electron detection angle was $\Theta = 70°$ with respect to the surface normal. Oxygen dosage (10 L O_2) was performed at 80 K. (A) O1s and V2p XPS spectra. (B) valence band spectra. At the top a spectrum of the vanadyl terminated surface is shown in panel (B). Reproduced from Ref. [32].

of the V2p levels to higher binding energy [Fig. 2(A), spectra (β)–(ε)] since it is known that the V2p binding energy increases with increasing vanadium oxidation state [36–38].

If the sample is warmed up to 610 K vanadyl groups form on the surface as is obvious from a comparison of the two top spectra in Fig. 2(B): the valence band of the annealed, oxygen-dosed sample is very similar to that of the vanadyl terminated sample. The peak at about 5 eV has been assigned to vanadyl groups [32]. The valence band spectra recorded for temperatures between 80 and 210 K [Fig. 2(B), spectra (β)–(ε)] are noticeably different from the valence band spectrum of the vanadyl terminated surface shown at the top. This means that the oxygen species on the surface are not just vanadyl groups at low temperature. There are also indications that the effective oxidation state of the surface vanadium atoms is higher in Fig. 2(B), spectra (β)–(ε) than in the spectra of the vanadyl terminated surface [spectra (ζ) and (η)] since the intensity of the V3d emission is smaller.

Fig. 3 displays IRAS spectra taken from the reduced $V_2O_3(0001)$ surface after exposure to O_2 at 90 K as a function of the annealing temperature. At low temperature two bands at 951 and 1030 cm^{-1} are observed. The band at 1030 cm^{-1} is assigned to vanadyl species [32]. The vanadyl feature increases in intensity and shifts to higher frequency (up to 1040 cm^{-1}) upon annealing above 170 K, while the band at 951 cm^{-1} vanishes. The 951 cm^{-1} band falls into the 900–1100 cm^{-1} range [15], which is typical of peroxo (O_2^{2-}) surface species, while superoxide (O_2^-) species have characteristic vibrations in the range of 1100–1150 cm^{-1} [15]. Based on this knowledge we propose the existence of peroxo species on the $V_2O_3(0001)$ surface.

To support this assignment, we performed spin-polarized DFT calculations on the structure and vibrational properties of oxygen species adsorbed on $V_2O_3(0001)$. The surface was modelled by a finite cluster and by a periodic slab (see Fig. 4). By cleaving the bulk V_2O_3 crystal along the (0001) direction a slab of V_2O_3 composition was obtained that consists of twelve vanadium layers and is single-metal terminated. The finite cluster cut out of this slab has the composition V_8O_{12} (D_{3d} symmetry). In terms of the metal and oxygen layers of the corundum structure it consists of four vanadium and two oxygen layers with only one vanadium atom in the top and bottom vanadium layers. A similar model ($O{=}VAl_7O_{12}$) was successfully used previously for vanadyl species on the α-alumina (0001) surface [39].

In the optimized structure of the O_2/cluster complex the O_2 ligand is aligned parallel to the surface in an η^2-mode with an O–O distance of 144.4 pm and V–O distances of 182.7 pm, whereas in the periodic structure the O_2 species are slightly tilted with respect to the surface plane in accord with the local C_{3V} symmetry of the VO_3 surface unit (upper part of Fig. 4). The V–O distances are 180.3 and 183.6 pm and the O–O distance is 143.6 pm (see Fig. 4). At the vanadium atoms of the $V_2O_3(0001)$ surface there are two electrons with parallel spin in d-states. On formation of a peroxo species these spins pair with the two spins of the

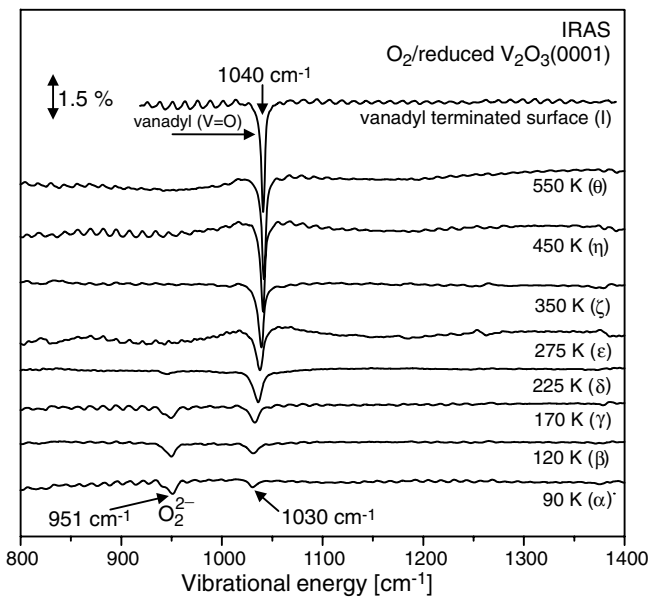

Fig. 3. IRAS spectra of oxygen on reduced $V_2O_3(0001)$ as a function of temperature after dosing 15 L O_2 at 90 K. At the top a spectrum of the vanadyl terminated $V_2O_3(0001)$ surface is shown. All spectra are referenced to a spectrum of the reduced surface, i.e. the spectra shown in this figure result from a division of an absorption spectrum of an oxygen covered or vanadyl terminated surface by a spectrum of the reduced surface.

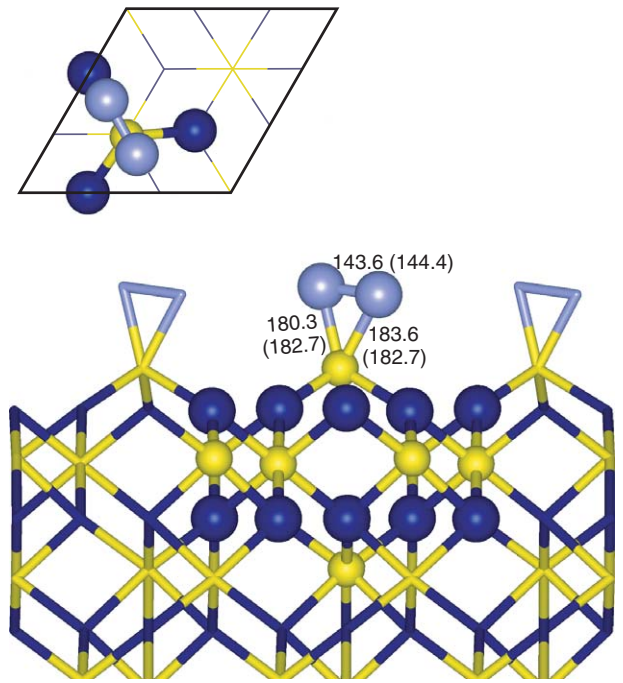

Fig. 4. Side view of the O_2^{2-} species on the $V_2O_3(0001)$ surface. Vanadium atoms are yellow, oxygen atoms from the slab are dark blue, whereas those from the O_2^{2-} are light blue. Balls and sticks are used to indicate the cluster model cut out from the $V_2O_3(0001)$ surface. Bond lengths for the slab and the cluster (in parentheses) are given in pm. The top view (upper part) shows the orientation of the O_2^{2-} species relative to the VO_3 surface unit.

triplet oxygen and the number of unpaired spins on the V_2O_3 surface is lowered by 2. In the covalent picture this corresponds to formation of two V–O bonds, whereas in the ionic picture two electrons are transferred from V d-orbitals into antibonding orbitals of O_2, which explains the elongation of the O–O bond compared to its value in O_2 (122.3 pm).

Using the cluster model, a search for a superoxo species was also made. Compared to the peroxo species, the number of unpaired spins is larger by 2, because in the superoxo species O_2 makes only one bond with the surface and only one of the d-electrons on vanadium pairs with one of the spins of the oxygen triplet. A local minimum has been found for a superoxo species with an O–O distance of 133.7 pm and V–O distances of 197.5 and 208.8 pm, but at significantly higher energies (1.01 eV higher than peroxo).

The frequency calculations for the peroxo species on $V_2O_3(0001)$ yield a quite intense IR-active mode at 904 cm^{-1} (cluster model) or 960 cm^{-1} (periodic model). It corresponds to the displacements indicated in Fig. 5, namely the O–O valence stretching of the peroxo species. In addition, calculations for the vanadyl terminated V_2O_3 surface were performed and V=O stretching frequencies of 977 cm^{-1} (cluster model) and 1027 cm^{-1} (periodic) were obtained. To correct for the systematic error of DFT and for neglected anharmonicity we applied a scaling factor [40] of 0.95812. The latter has been derived for the $V_4O_{11}^-$ anion (PBE/TZVP) for which experimental gas phase spectra are available [41]. Comparison between both models indicates a systematic underestimation of the vibrational frequencies by the cluster model, which does not come as a surprise given its very limited size. Nevertheless, the frequency shift between the vanadyl and the peroxo surface species is well reproduced even with the cluster model. Also the intensity ratio peroxo mode/vanadyl mode is very similar for the cluster (0.71) and the periodic model (0.65) and in qualitative agreement with the experimental spectra.

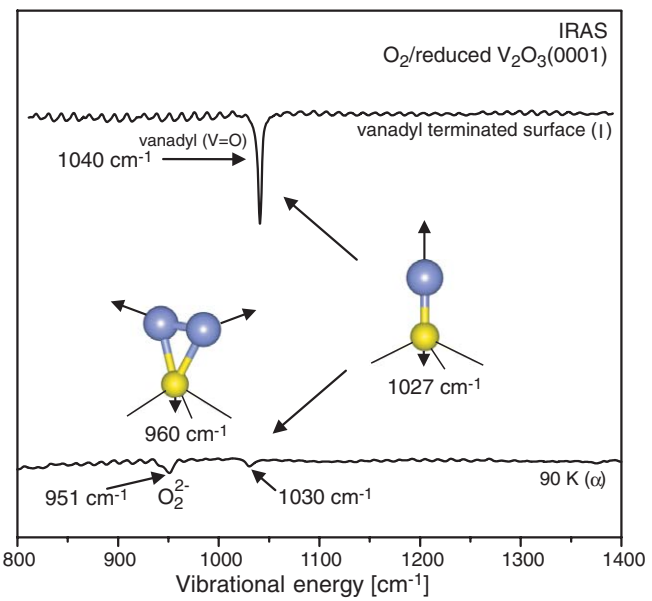

Fig. 5. Calculated harmonic vibrational frequencies (scaled, in cm^{-1}) for the periodic model.

The experimental vibrational energy of 951 cm^{-1} is in excellent agreement with the 960 cm^{-1} predicted for the peroxo species with the periodic model. There remains one question, however. With IRAS only modes will be observed that are connected with changes of the dipole moment perpendicular to the surface. Why is the O–O valence stretching mode connected with a changing dipole moment although it is almost parallel to the surface (Fig. 5)? The DFT calculations tell us that the peroxo bond represents a $V^{\delta+}$–$O_2^{\delta-}$ dipole perpendicular to the surface. This dipole changes with motions along the O–O stretching mode, firstly because this mode has also a component that changes the V–O bond distances (Fig. 5), and secondly and more importantly because the charge separation between V and O_2 changes with the O–O distance. It gets smaller with decreasing distance and larger with increasing distance. Based on these computational results, the band at 951 cm^{-1} is unequivocally assigned to η^2-peroxo species on $V_2O_3(0001)$ surfaces. A similar explanation was put forward by Gustafsson et al. to explain the non-vanishing intensity of the O–O vibration in IRAS spectra of physisorbed O_2 molecules on Pt(111) [42].

The calculated binding energies (periodic model) for the peroxo species (3.56 eV/O_2 molecule) and for the vanadyl oxygen (4.08 eV/$\frac{1}{2}O_2$ molecule) are also in line with the observed changes of the IRAS spectrum with increasing temperature.

For O_2 adsorption on the isostructural (0001) surface of Cr_2O_3 the same behavior has been observed and the low temperature surface species which was found to exhibit an IR absorption at 963 cm^{-1} [9,10] is most likely also a peroxo species.

Thermal desorption data (not shown here) of an oxygen dosed surface measured for mass 32 (O_2) and mass 16 (O) exhibit only weak desorption signals. The intensities observed in these data are about a factor of 100–200 weaker than the signal observed with the same setup for a monolayer of molecular propane desorbing from the surface. Of course, the pumping speeds for molecular propane and oxygen are somewhat different and the probabilities for sticking to the walls are likely not identical, but it is hard to imagine that these differences account for intensities different by a factor of 100–200. Thus it may be assumed that the structures observed in the TDS data are due to desorption of some minority species, possibly interacting with surface defects or to a reaction path with low probability.

This observation essentially means that nearly all of the oxygen atoms of the O_2^{2-} groups adsorbed on the surface at low temperature are used for the formation of vanadyl groups. A comparison of the intensities of the vanadyl vibrations in the two topmost spectra in Fig. 3 clearly shows that the warming up of the oxygen-covered surface

leads to a surface which is fully covered by vanadyl groups. Since one surface vanadium atom binds one oxygen atom to form vanadyl groups, the coverage of the surface vanadium atoms with O_2^{2-} should be about 0.5, i.e only every second surface vanadium atoms carries an O_2^{2-} group according to the TDS data.

On the other hand, the valence band spectra shown in Fig. 2(B) are indicative of a rather high O_2^{2-} coverage on the surface. In the temperature range where the surface is covered by O_2^{2-} the V3d intensity is even smaller than in the case of the vanadyl terminated surface (the two topmost spectra). This suggests that the average effective oxidation state of the surface vanadium atoms is even higher for O_2^{2-} coverage than for vanadyl termination which is somewhat at variance with the limited coverage (~0.5) concluded from the TDS data. It is actually not really clear why only every second vanadium atom at the surface should carry a O_2^{2-} molecule since these molecules bond strongly to the surface vanadium atoms (3.56 eV per O_2 molecule as discussed before). Strong repulsive lateral interactions would be a possible explanation, but in view of the large lateral distance of the surface vanadium atoms (5.1 Å according to Ref. [43], 4.9 Å according to the DFT calculations, this work) and the strong vanadium to O_2^{2-} bond it is unlikely that this explanation really holds. Indeed, after removing every second peroxo species (peroxo coverage 0.5) the binding energy per O_2 molecule increases by 0.14 eV only. Thus the situation with respect to the O_2^{2-} coverage remains somewhat unclear but it may be stated that the coverage is likely between 0.5 and 1.

HREELS spectra are shown in Fig. 6. The spectrum of the clean reduced $V_2O_3(0001)$ surface exhibits a number of losses due to the optical phonons of the oxide. Adsorption of oxygen on the reduced $V_2O_3(0001)$ surface at 90 K leads to additional losses at 950 and 1040 cm^{-1}, in good agreement with the above IRAS results. Moreover, a shoulder is found at about 765 cm^{-1} for the oxygen dosed surface and the vanadyl terminated surface but not for the reduced surface. According to the DFT calculations this feature may be assigned to a surface localized mode which exhibits sizeable intensity for the vanadyl terminated and peroxo covered surface, but not for the reduced surface. In addition, its energy shifts to slightly higher wavenumbers from reduced (681 cm^{-1}) to vanadyl terminated (690 cm^{-1}) and peroxo covered surfaces (711 cm^{-1}). Table 1 shows calculated vibrational energies and intensities in comparison to bulk phonons. The surface mode is a V–O stretching mode which involves the atoms of the oxygen layer just beneath the surface terminating vanadium layer. For the peroxo covered surface it is also coupled to motions of the peroxo O atoms, while for the vanadyl terminated surface it extends further into the interior of the slab and includes also motions of atoms of the subsequent vanadium layers. For the metal terminated and the vanadyl terminated surface this mode has already been described by Kresse et al. [44].

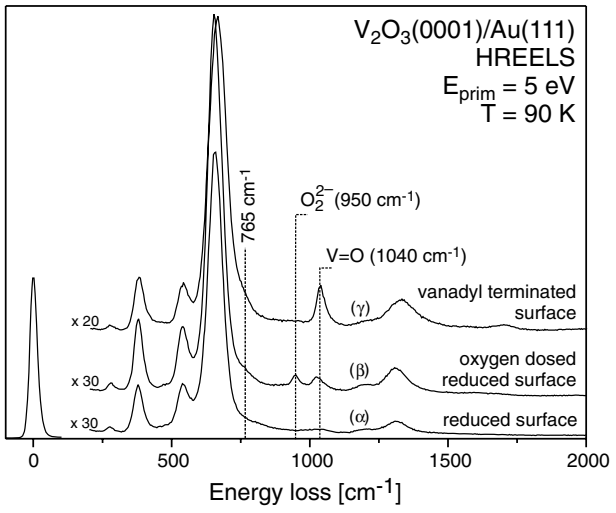

Fig. 6. HREELS spectra of vanadyl terminated, reduced, and oxygen dosed reduced $V_2O_3(0001)$/Au(111). Before spectrum (β) was recorded, the reduced surface was dosed with 15 L of oxygen at 90 K. All spectra were recorded at 90 K.

Table 1
Highest vibrational energies (in cm^{-1}) and relative intensities (in brackets, dipole derivatives perpendicular to the surface) for bulk V_2O_3, vanadium terminated, vanadyl terminated and peroxo terminated $V_2O_3(0001)$ surfaces

Bulk V_2O_3	Vanadium terminated $V_2O_3(0001)$	Vanadyl terminated $V_2O_3(0001)$	Peroxo terminated $V_2O_3(0001)$
		1027[a] (1.00)	960[a] (0.65)
			711 (0.14)
	681 (<0.01)	690 (0.08)	668 (<0.01)
610	625	655	647
574	591	595	595

[a] Scaled, see context of Fig. 5.

5. Summary

By applying a variety of surface sensitive experimental techniques and density functional theory we have investigated the adsorption of oxygen on reduced $V_2O_3(0001)$ under UHV conditions. The experimental data show that oxygen interacts strongly with this surface. Adsorption at 90 K results in the formation of a negatively charged adsorbed oxygen species which was identified as peroxo, O_2^{2-} using density functional theory. In addition also a small coverage of vanadyl groups was detected. Upon warming up the O_2^{2-} molecular ions dissociate and the resulting oxygen atoms bond to the surface vanadium atoms, forming vanadyl groups. From TDS data and valence band spectra we conclude that the coverage of the surface vanadium atoms with O_2^{2-} atoms at low temperature should be between 0.5 and 1.

Acknowledgements

This work was funded by the Deutsche Forschungsgemeinschaft through their Sonderforschungsbereich 546 'Transition Metal Oxide Aggregates'. The Fonds der

Chemischen Industrie is gratefully acknowledged for financial support.

References

[1] K. Hermann, M. Witko, Theory of physical and chemical behaviour of transition metal oxides: vanadium and molybdenum oxides, in: D.A. King, D.P. Woodruff (Eds.), Oxide Surfaces, The Chemical Physics of Solid Surfaces, vol. 9, Elsevier, 2001, p. 136.
[2] S. Surnev, M.G. Ramsey, F.P. Netzer, Prog. Surf. Sci. 73 (2003) 117.
[3] H.H. Kung, Oxidative dehydrogenation of light (C2 to C6) alkanes, in: D. Riley, H. Pines, W. Haag (Eds.), Advances in Catalysis, 40, Elsevier, 1994, p. 1.
[4] A. Bielański, J. Haber, Oxygen in Catalysis, Marcel Dekker, New York, 1991.
[5] M. Iwamoto, J.H. Lunsford, J. Phys. Chem. 84 (1980) 3079.
[6] V.E. Henrich, Rep. Prog. Phys. 48 (1985) 1481.
[7] A.A. Davydov, Infrared Spectroscopy of Adsorbed Species on the Surfaces of Transition Metal Oxides, Wiley & Sons, Chichester, United Kingdom, 1990.
[8] C. Louis, T.L. Chang, M. Kermarec, T.L. Van, J.M. Tatibouët, M. Che, Coll. Surf. A 72 (1993) 217.
[9] H.-J. Freund, B. Dillmann, O. Seiferth, G. Klivenyi, M. Bender, D. Ehrlich, I. Hemmerich, D. Cappus, Catalysis Today 32 (1996) 1.
[10] B. Dillmann, F. Rohr, O. Seiferth, G. Klivenyi, M. Bender, K. Homann, I.N. Yakovkin, D. Ehrlich, M. Bäumer, H. Kuhlenbeck, H.-J. Freund, Faraday Disc. 105 (1996) 295.
[11] M. Haneda, T. Mizushima, N. Kakuta, J. Chem. Soc. Faraday Trans. 91 (1995) 4459.
[12] D. Barreca, F. Morazzoni, G.A. Rizzi, R. Scotti, E. Tondello, Phys. Chem. Chem. Phys. 3 (2001) 1743.
[13] T. Kawabe, K. Tabata, E. Suzuki, Y. Yamaguchi, Y. Nagasawa, J. Phys. Chem. B 105 (2001) 4239.
[14] V.V. Pushkarev, V.I. Kovalchuk, J.L. d'Itri, J. Phys. Chem. B 108 (2004) 5341.
[15] N. Sheppard, in: R.F. Willis (Ed.), Vibrational Spectroscopy of Adsorbates, Springer Series in Chemical Physics, vol. 15, Springer Verlag, Berlin, 1980, p. 165.
[16] M. Che, A.J. Tench, Characterization and reactivity of mononuclear oxygen species on oxide surfaces, in: D.D. Eley, H. Pines, P.B. Weisz (Eds.), Advances in Catalysis, vol. 31, Elsevier, 1982, p. 77.
[17] M. Che, A.J. Tench, Characterization and reactivity of molecular oxygen species on oxide surfaces, in: D.D. Eley, H. Pines, P.B. Weisz (Eds.), Advances in Catalysis, vol. 32, Elsevier, 1983, p. 1.
[18] C. Li, K. Domen, K. Maruya, T. Onishi, J. Am. Chem. Soc. 111 (1989) 7683.
[19] V.M. Bermudez, V.H. Ritz, Chem. Phys. Lett. 73 (1980) 160.
[20] J.P.S. Badyal, X. Zhang, R.M. Lambert, Surf. Sci. 225 (1990) L15.
[21] A.F. Carley, S.D. Jackson, M.W. Roberts, J. O'Shea, Chem. Phys. Lett. 454–456 (2000) 141.
[22] J.P. Perdew, J.A. Chevary, S.H. Vosko, K.A. Jackson, M.R. Pederson, D.J. Singh, C. Fiolhais, Phys. Rev. B 46 (1992) 6671.
[23] G. Kresse, J. Furthmüller, Comput. Mater. Sci. 6 (1996) 15.
[24] G. Kresse, J. Furthmüller, Phys. Rev. B 54 (1996) 11169.
[25] P.E. Blöchl, Phys. Rev. B 50 (1994) 17953.
[26] G. Kresse, D. Joubert, Phys. Rev. B 59 (1999) 1758.
[27] R. Ahlrichs, M. Bär, M. Häser, H. Horn, C. Kölmel, Chem. Phys. Lett. 162 (1989) 165.
[28] O. Treutler, R. Ahlrichs, J. Chem. Phys. 102 (1995) 346.
[29] A. Schäfer, C. Huber, R. Ahlrichs, J. Chem. Phys. 100 (1994) 5829.
[30] J.P. Perdew, K. Burke, M. Ernzerhof, Phys. Rev. Lett. 77 (1996) 3865.
[31] P. Deglmann, F. Furche, R. Ahlrichs, Chem. Phys. Lett. 362 (2002) 511.
[32] A.-C. Dupuis, M. Abu Haija, B. Richter, H. Kuhlenbeck, H.-J. Freund, Surf. Sci. 539 (2003) 99.
[33] J. Schoiswohl, M. Sock, S. Surnev, M.G. Ramsey, F.P. Netzer, G. Kresse, J.N. Andersen, Surf. Sci. 555 (2004) 101.
[34] S. Guimond, M. Naschitzki, M. Abu Haija, H. Kuhlenbeck, H.-J. Freund, in preparation.
[35] S. Guimond, M. Abu Haija, S. Kaya, J. Lu, J. Weissenrieder, S.K. Shaikhutdinov, H. Kuhlenbeck, H.-J. Freund, J. Döbler, J. Sauer, Top. Catal., submitted for publication.
[36] G.A. Sawatzky, D. Post, Phys. Rev. B 20 (1979) 1546.
[37] J. Mendialdua, R. Casanova, Y. Barbaux, J. Electron Spectrosc. Relat. Phenom. 71 (1995) 249.
[38] G. Silversmit, D. Depla, H. Poelman, G.B. Marin, R.D. Gryse, J. Electron Spectrosc. Relat. Phenom. 135 (2004) 167.
[39] N. Magg, B. Immaraporn, J.B. Giorgi, T. Schroeder, M. Bäumer, J. Döbler, Z. Wu, E. Kondratenko, M. Cherian, M. Baerns, P.C. Stair, J. Sauer, H.-J. Freund, J. Catal. 226 (2004) 88.
[40] A.P. Scott, L. Radom, J. Chem. Phys. 100 (1996) 16502.
[41] G. Santambrogio, M. Brümmer, L. Wöste, J. Sauer, G. Meijer, K.R. Asmis, in preparation.
[42] K. Gustafsson, S. Andersson, J. Chem. Phys. 120 (2004) 7750.
[43] R.W.G. Wyckoff, Crystal Structures, second ed., Wiley Interscience, New York, 1965.
[44] G. Kresse, S. Surnev, J. Schoiswohl, F.P. Netzer, Surf. Sci. 555 (2004) 118.